

Coherent phase control of orbital-angular-momentum light-induced torque in a double-tripod atom-light coupling scheme

Hamid R. Hamedī^{1,*}, Viačeslav Kudrišov^{1,†}, Mažena Mackoit Sinkevičienė^{1,‡}, and Julius Ruseckas^{1,§}

¹*Institute of Theoretical Physics and Astronomy, Vilnius University, Saulėtekio 3, Vilnius LT-10257, Lithuania*

²*Baltic Institute of Advanced Technology, 01403 Vilnius, Lithuania*



(Received 20 August 2025; accepted 3 December 2025; published 18 December 2025)

We investigate a phase-controllable mechanism for generating optical torque in a five-level double-tripod (DT) atom-light coupling scheme interacting with four strong coherent control fields as well as two weak optical vortex probe beams carrying orbital angular momentum (OAM). The spatial phase gradients of the OAM-carrying probes induce a quantized torque that is transferred to the atoms, rotating them and generating a directed atomic flow within an annular geometry. Analytical solutions of the optical Bloch equations under steady-state conditions show that the induced torque and resulting rotational motion exhibit high sensitivity to phase variations. We show that the DT system coherently reconfigures into either coupled- Λ or double- Λ schemes depending on the relative phases, with each configuration exhibiting distinct quantized torque characteristics. This enables precise phase control of the atomic current flow, with potential applications in quantum control, precision measurement, and quantum information processing.

DOI: [10.1103/nbx8-l3v4](https://doi.org/10.1103/nbx8-l3v4)

I. INTRODUCTION

The interaction between coherent light and atomic systems leads to a wide range of intriguing quantum phenomena, driven by atomic coherences and light-induced control of medium properties [1–4]. One of the most extensively studied effects in this domain is electromagnetically induced transparency (EIT) [5–7], a quantum interference phenomenon that allows an otherwise opaque medium to become transparent under specific conditions. Electromagnetically induced transparency plays a crucial role in slow light experiments, where the group velocity of light is significantly reduced due to the presence of atomic coherence [8–13]. Slow light and EIT have been studied in three- and four-level systems, particularly in Λ and tripod configurations [9,10,14,15], each employing distinct pathways for coherence-based control of light propagation. Moving beyond these schemes, the extension of EIT to more complex multilevel atomic systems [16] has opened new avenues for enriched quantum dynamics and enhanced light-matter interaction control. Among these, the double-tripod (DT) system [11,17] has gained particular attention due to its unique coherence properties and relevance to nonlinear optics and quantum information processing. Consisting of two upper and three lower atomic levels, coupled by six optical fields in total, the DT system represents a highly controllable quantum medium. A particularly interesting effect in the DT system is spinor slow light [11], which introduces additional internal degrees of freedom for controlling light-matter interactions and

has implications for structured light dynamics in multilevel atomic ensembles.

In parallel with EIT and slow light, a fundamentally important concept in modern quantum optics is the orbital angular momentum (OAM) of light [18,19]. Orbital-angular-momentum-carrying vortex beams possess a helical wave front and can impart quantized angular momentum to atoms, leading to novel interactions [20]. A demonstration by Radwell *et al.* [21] showed that the coherent coupling between OAM-carrying light and atomic ensembles can lead to spatially dependent EIT. This was later extended theoretically to more complex atomic schemes, where the interaction of vortex beams with combined tripod and Λ -type configurations enabled the coherent transfer of OAM to a probe field in a resonant medium [22]. The influence of OAM on atomic systems has been investigated in various contexts, including azimuthally dependent EIT [21–23], direct OAM transfer between light and atomic states [24–27], magnetometry [28], and mechanical effects induced by structured light [29–31]. These interactions of OAM with atomic ensembles introduce additional degrees of freedom to light-matter coupling, offering enhanced control over atomic coherence and state manipulation and opening pathways for novel effects applicable to quantum computation, quantum information storage, and quantum teleportation [32,33]. This flexibility enables enhanced manipulation of quantum states, tailored optical responses, and new coherence phenomena, all essential for understanding the complex behavior of structured light fields in multilevel atomic systems.

A particularly fascinating effect of OAM-carrying light is the generation of optical torque in atomic media, where OAM light fields transfer angular momentum to atoms, inducing mechanical rotation or atomic motion [29–31,34]. A previous study investigated torque effects in a three-level Λ system

*Contact author: hamid.hamedi@tfai.vu.lt

†Contact author: viaceslav.kudrišov@ff.vu.lt

‡Contact author: mazena.mackoit-sinkevičiene@ff.vu.lt

§Contact author: julius.ruseckas@gmail.com

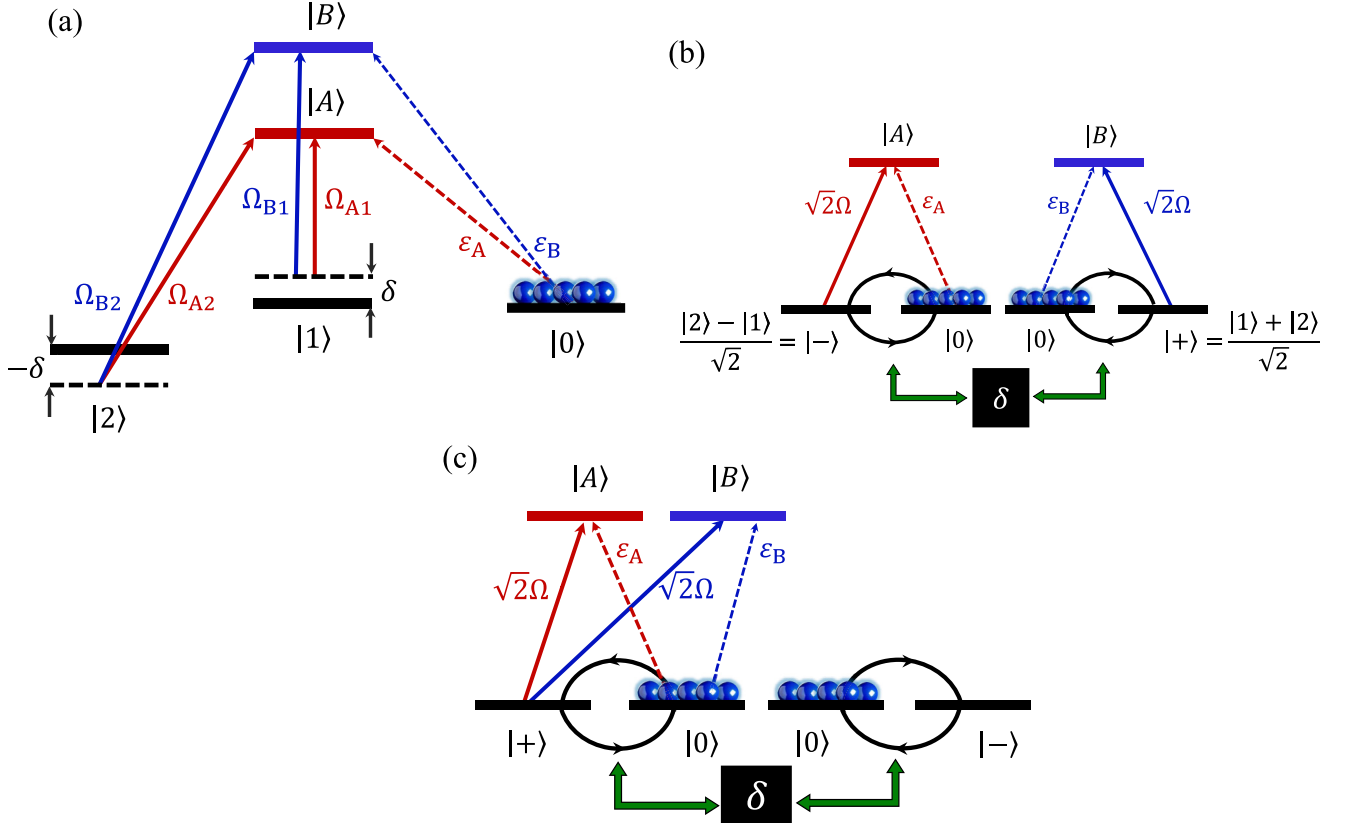


FIG. 1. (a) Schematic of the double-tripod configuration, in which three ground states $|0\rangle$, $|1\rangle$, and $|2\rangle$ are coupled to two excited states $|A\rangle$ and $|B\rangle$ via two probe fields ε_A and ε_B , along with four strong control fields Ω_{A1} , Ω_{A2} , Ω_{B1} , and Ω_{B2} . (b) Representation of two coupled- Λ systems with a common effective Rabi frequency $\sqrt{2}\Omega$. This model is equivalent to the DT system. When all four coupling fields have equal amplitude Ω , the relative phase is $\phi = \pi$ and the additional phase is $\theta = 0$. The two-photon detuning δ establishes a coupling between the two effective Λ systems. (c) Equivalent transition diagram for the DT system at $\phi = 0$ and $\theta = 0$, where the structure combines a double- Λ system with a two-ground-state system. The coupling between the subsystems is mediated by ground-state coherences.

driven by two OAM beams, revealing complex exchanges of angular momentum between light and matter [31]. In that case, the magnitude of the induced torque was determined solely by the beam amplitudes and the detuning of the fields. In this work, we propose phase control of the optical torque as a new degree of freedom in a more intricate five-level DT scheme. The DT system interacts with four strong control fields and two weak OAM-carrying probe fields, where the multiple excitation pathways make it an effective platform for exploring the mechanical impact of structured light. Importantly, the strong control fields form a closed loop, and their relative phase can directly influence the optical response of the probe fields. This feature is absent in a double- Λ configuration [26], where OAM probe beams are part of the closed loop. Because the intensity of OAM beams vanishes at the vortex core, the loop is effectively broken at those points, and no well-defined relative phase can be established, rendering phase control of the induced torque impossible in that setting. In contrast, in the DT scheme the OAM probe beams that generate torque lie outside the closed loop formed entirely by nonvortex control fields. As a result, the loop remains intact everywhere, independent of the probe's vortex structure, making it possible to exert phase control over the probe properties, including the induced optical torque. We further show that by adjusting the relative phases of the

control fields, the DT system can be coherently reconfigured into either coupled- Λ subsystems or an effective double- Λ configuration. This reconfigurability enables tunable optical torque and controlled rotational motion of atoms, offering a mechanism for precise manipulation of atomic currents in annular geometries. Understanding the role of torque in this regime opens new avenues for controlling atomic motion and engineering advanced quantum optical systems.

II. THEORETICAL MODEL

A. System

We investigate the interaction between light and matter in an atomic ensemble using a five-level DT configuration, as illustrated in Fig. 1(a). The atomic system comprises three ground states $|0\rangle$, $|1\rangle$, and $|2\rangle$ along with two excited states $|A\rangle$ and $|B\rangle$. Two weak probe fields ε_A and ε_B drive the transitions $|0\rangle \leftrightarrow |A\rangle$ and $|0\rangle \leftrightarrow |B\rangle$, respectively. In addition, four coherent control fields with Rabi frequencies Ω_{A1} , Ω_{A2} , Ω_{B1} , and Ω_{B2} mediate dipole-allowed transitions $|A\rangle \leftrightarrow |1\rangle$, $|A\rangle \leftrightarrow |2\rangle$, $|B\rangle \leftrightarrow |1\rangle$, and $|B\rangle \leftrightarrow |2\rangle$, respectively, forming a closed-loop coherent subsystem within the DT structure. This loop enables quantum interference and coherent control over the internal dynamics of the atomic ensemble, making the system highly sensitive to the relative phases of the applied control fields.

The interaction Hamiltonian of the system, expressed in units where $\hbar = 1$, is given by

$$\begin{aligned} H = & (-\varepsilon_A |A\rangle\langle 0| - \varepsilon_B |B\rangle\langle 0| - \Omega_{A1}|A\rangle\langle 1| - \Omega_{A2}|A\rangle\langle 2| \\ & - \Omega_{B1}|B\rangle\langle 1| - \Omega_{B2}|B\rangle\langle 2|) + \text{H.c.} - \delta(|2\rangle\langle 2| - |1\rangle\langle 1|), \end{aligned} \quad (1)$$

where δ represents the two-photon detuning, assigning an energy shift of $+\delta$ to state $|1\rangle$ and $-\delta$ to $|2\rangle$. We treat the interaction of the fields with the atoms using the electric dipole approximation. The detuning of the probe field appears in the full Hamiltonian as a term of the form $\Delta|0\rangle\langle 0|$; however, for simplicity in the subsequent analysis, we omit this term in the current presentation.

To simplify the dynamics, we introduce the bright and dark states for each subsystem coupled (bright) or decoupled (dark) from the states $|A\rangle$ and $|B\rangle$, respectively. For the subsystem coupled to $|A\rangle$, the bright and dark states are defined as

$$|\mathcal{B}_A\rangle = \frac{\Omega_{A1}^*|1\rangle + \Omega_{A2}^*|2\rangle}{\Omega_A}, \quad (2)$$

$$|\mathcal{D}_A\rangle = \frac{\Omega_{A2}|1\rangle - \Omega_{A1}|2\rangle}{\Omega_A}, \quad (3)$$

where $\Omega_A = \sqrt{|\Omega_{A1}|^2 + |\Omega_{A2}|^2}$. Similarly, for the subsystem coupled to $|B\rangle$, the bright and dark states are

$$|\mathcal{B}_B\rangle = \frac{\Omega_{B1}^*|1\rangle + \Omega_{B2}^*|2\rangle}{\Omega_B}, \quad (4)$$

$$|\mathcal{D}_B\rangle = \frac{\Omega_{B2}|1\rangle - \Omega_{B1}|2\rangle}{\Omega_B}, \quad (5)$$

with $\Omega_B = \sqrt{|\Omega_{B1}|^2 + |\Omega_{B2}|^2}$. Here Ω_A and Ω_B represent the effective Rabi frequencies coupling the states $|A\rangle$ and $|B\rangle$ to their respective bright states. By expressing the system in the new basis $\{|\mathcal{B}_A\rangle, |\mathcal{D}_A\rangle, |\mathcal{B}_B\rangle, |\mathcal{D}_B\rangle\}$, the Hamiltonian from Eq. (1) takes a simplified form once the dark states are decoupled,

$$\begin{aligned} H = & (-\varepsilon_A |A\rangle\langle 0| - \varepsilon_B |B\rangle\langle 0| - \Omega_A |A\rangle\langle \mathcal{B}_A| - \Omega_B |B\rangle\langle \mathcal{B}_B|) \\ & + \text{H.c.} - \delta(C_B |\mathcal{B}_A\rangle\langle \mathcal{B}_A| + C_D |\mathcal{D}_A\rangle\langle \mathcal{D}_A| \\ & + C_X |\mathcal{B}_A\rangle\langle \mathcal{D}_A| + C_X^* |\mathcal{D}_A\rangle\langle \mathcal{B}_A|), \end{aligned} \quad (6)$$

where the coefficients are introduced as

$$C_B = |\Omega_{A2}|^2 - |\Omega_{A1}|^2, \quad (7)$$

$$C_D = -C_B, \quad (8)$$

$$C_X = -\frac{\Omega_{A1}\Omega_{A2} + \Omega_{A1}^*\Omega_{A2}^*}{|\Omega_{A1}|^2 + |\Omega_{A2}|^2}. \quad (9)$$

B. Induced torque on DT atoms

Let us now consider that the two weak probe fields ε_A and ε_B are spatially inhomogeneous, counterpropagating beams along the z coordinate. These probe fields are expressed as

$$\varepsilon_A = \Omega_{A0} e^{i\Phi_{A0}(\mathbf{R})}, \quad (10)$$

$$\varepsilon_B = \Omega_{B0} e^{il\Phi_{B0}(\mathbf{R})}, \quad (11)$$

where the spatial phase profiles are given by

$$\Phi_{A0}(\mathbf{R}) = -l\varphi + kz, \quad (12)$$

$$\Phi_{B0}(\mathbf{R}) = -l\varphi - kz. \quad (13)$$

Here k is the wave number, l denotes OAM or topological charge, and φ is the azimuthal angle in cylindrical coordinates. We consider the effects arising near the beam waist, which is situated in the plane $z = 0$. The amplitudes of the probe fields, corresponding to the Rabi frequencies Ω_{A0} and Ω_{B0} , are modeled as doughnut-shaped Laguerre-Gaussian (LG) beams with a shared radial profile

$$\Omega_{A0} = |\Omega_{A0}|G(r), \quad (14)$$

$$\Omega_{B0} = |\Omega_{B0}|G(r), \quad (15)$$

where the spatial mode function is defined as $G(r) = (\frac{r}{w})^{|l|} e^{-r^2/w^2}$, with r the radial coordinate and w the beam waist, and $|\Omega_{A0}|$ and $|\Omega_{B0}|$ represent the strengths of the position-dependent beams.

We will derive the expression for the optical force using the semiclassical approximation. Since only spatially varying terms in the Hamiltonian can contribute to the force, the force arises solely from the spatial dependence embedded in ε_A and ε_B . Therefore, the relevant part of the Hamiltonian for force derivation reduces to

$$H_{\text{probe}} = -\varepsilon_A |A\rangle\langle 0| - \varepsilon_B |B\rangle\langle 0| - \varepsilon_A^* |0\rangle\langle A| - \varepsilon_B^* |0\rangle\langle B|. \quad (16)$$

Correspondingly, the expectation value of this part is

$$\langle H_{\text{probe}} \rangle = -\varepsilon_A \sigma_{0A} - \varepsilon_B \sigma_{0B} - \varepsilon_A^* \sigma_{A0} - \varepsilon_B^* \sigma_{B0}, \quad (17)$$

where $\sigma_{ij} = \langle i|\sigma|j\rangle$ represents the density-matrix element in the laboratory frame. Following the principles underlying Ehrenfest's theorem [35], the optical force is

$$\mathbf{F} = \sigma_{0A} \nabla \varepsilon_{A0} + \sigma_{0B} \nabla \varepsilon_{B0} + \sigma_{A0} \nabla \varepsilon_{A0}^* + \sigma_{B0} \nabla \varepsilon_{B0}^*. \quad (18)$$

By substituting Eqs. (10) and (11) into Eq. (18) and applying the slowly varying envelope approximation (SVEA) together with the rotating-wave approximation (RWA) [2], the resulting expression for the optical force becomes

$$\begin{aligned} \mathbf{F} = & i\Omega_{A0}(\rho_A^* - \rho_A)\nabla\Phi_{A0} + i\Omega_{B0}(\rho_B^* - \rho_B)\nabla\Phi_{B0} \\ = & 2[\Omega_{A0}\text{Im}(\rho_A)\nabla\Phi_{A0}(\mathbf{R}) + \Omega_{B0}\text{Im}(\rho_B)\nabla\Phi_{B0}(\mathbf{R})]. \end{aligned} \quad (19)$$

Here we ignored the dipole force related to the gradients of the field intensities and consider only the resonance-radiation pressure related to the gradients of the phases. The quantities ρ_A and ρ_B are the coherences (off-diagonal elements of the density matrix) corresponding to the probe transitions $|0\rangle \leftrightarrow |A\rangle$ and $|0\rangle \leftrightarrow |B\rangle$, respectively. In deriving Eq. (19) we assume that the many-body wave function of the trapped atomic ensemble can be approximated as a product of identical single-particle wave functions [30], implying that each atom experiences the same light-induced force. Moreover, each single-atom wave function is taken to be separable into internal and center-of-mass components. Consequently, as shown in Eq. (19), the force acting on the center-of-mass coordinate \mathbf{R} depends solely on the internal-state density-matrix elements.

The force expression featured in Eq. (19) depends on the gradients of spatial phases $\Phi_{A0}(\mathbf{R})$ and $\Phi_{B0}(\mathbf{R})$. Applying the

gradient operator in cylindrical coordinates

$$\nabla \Phi = \frac{\partial \Phi}{\partial r} \hat{r} + \frac{1}{r} \frac{\partial \Phi}{\partial \varphi} \hat{\varphi} + \frac{\partial \Phi}{\partial z} \hat{z} \quad (20)$$

to $\Phi_{A0}(\mathbf{R})$ and $\Phi_{B0}(\mathbf{R})$ given in Eqs. (12) and (13) and noting that $\Phi_{A0}(\mathbf{R})$ and $\Phi_{B0}(\mathbf{R})$ have no explicit dependence on r , we get

$$\nabla \Phi_{A0} = \left(-\frac{l}{r} \right) \hat{\varphi} + k \hat{z}, \quad (21)$$

$$\nabla \Phi_{B0} = \left(-\frac{l}{r} \right) \hat{\varphi} - k \hat{z}. \quad (22)$$

Substituting these gradients into Eq. (19), expanding, and rearranging the terms, we obtain

$$\begin{aligned} \mathbf{F} = 2 & \left(k[\Omega_{A0}\text{Im}(\rho_A) - \Omega_{B0}\text{Im}(\rho_B)]\hat{z} \right. \\ & \left. - \frac{l}{r}[\Omega_{A0}\text{Im}(\rho_A) + \Omega_{B0}\text{Im}(\rho_B)]\hat{\varphi} \right). \end{aligned} \quad (23)$$

To compute the torque exerted on the atomic center of mass about the beam axis, we extract the component of the cross product of the position vector \mathbf{R} and the force vector \mathbf{F} that is aligned with the axial (beam) direction. In cylindrical coordinates, the position vector \mathbf{R} possesses only radial and axial components, while the force \mathbf{F} contains contributions in the azimuthal and axial directions. Consequently, the only nonvanishing contribution to the torque about the beam axis comes from the cross product between the radial component of \mathbf{R} and the azimuthal component of \mathbf{F} . This yields a torque vector directed along \hat{z} . Thus, the induced torque on the center of mass of the DT atoms about the beam axis is given by

$$\mathbf{T} = \mathbf{r} \times \mathbf{F} = -2G^2(r)l\tau\hat{z}, \quad (24)$$

where we have defined the torque function

$$\begin{aligned} \tau &= |\Omega_{A0}| \left(\frac{|\Omega_{A0}|}{\Omega_{A0}} \text{Im}(\rho_A) \right) + |\Omega_{B0}| \left(\frac{|\Omega_{B0}|}{\Omega_{B0}} \text{Im}(\rho_B) \right) \\ &= \left(\frac{|\Omega_{A0}| \text{Im}(\rho_A) + |\Omega_{B0}| \text{Im}(\rho_B)}{G(r)} \right). \end{aligned} \quad (25)$$

The expression for torque in Eq. (24) clearly describes a discrete quantized torque that induces rotational motion in the atoms. Its magnitude increases with the topological charge l , and the torque exhibits a ringlike intensity profile that forms an optical dipole trap, drawing atoms toward regions of high intensity. The torque function given in Eq. (25) indicates its dependence on DT system parameters through the imaginary parts of the atomic coherences ρ_A and ρ_B . In particular, the relative phase among all control fields influences these coherences and thus affects the torque on the DT atoms. For illustrative purposes, we adopt this torque function in later sections. This phase dependence offers a means to dynamically control the torque, enabling the generation of a phase-sensitive, adjustable, intensity-driven circular atomic flow. In the following section, we derive explicit analytical solutions for the coherence terms ρ_A and ρ_B , demonstrating how the relative phase emerges in the equations, thereby shaping the induced torque and influencing atomic motion within the system.

C. Optical Bloch equations

In the DT system illustrated in Fig. 1(a), the evolution of the probe fields and the atomic coherences is described by the optical Bloch equations. For the optical coherences, we have [11]

$$\frac{\partial}{\partial t} \begin{bmatrix} \rho_A \\ \rho_B \end{bmatrix} = i\hat{\Omega} \begin{bmatrix} \rho_1 \\ \rho_2 \end{bmatrix} + \left(i\Delta - \frac{\Gamma}{2} \right) \begin{bmatrix} \rho_A \\ \rho_B \end{bmatrix} + i \begin{bmatrix} \Omega_{A0} \\ \Omega_{B0} \end{bmatrix}, \quad (26)$$

while for the ground-state coherences we have

$$\frac{\partial}{\partial t} \begin{bmatrix} \rho_1 \\ \rho_2 \end{bmatrix} = i\hat{\Omega}^\dagger \begin{bmatrix} \rho_A \\ \rho_B \end{bmatrix} + i(\Delta\hat{I} + \hat{\delta}) \begin{bmatrix} \rho_1 \\ \rho_2 \end{bmatrix}, \quad (27)$$

where we define the field interaction matrix $\hat{\Omega}$ and the two-photon detuning matrix $\hat{\delta}$ as

$$\hat{\Omega} = \begin{bmatrix} \Omega_{A1} & \Omega_{A2} \\ \Omega_{B1} & \Omega_{B2} \end{bmatrix}, \quad \hat{\delta} = \begin{bmatrix} \delta & 0 \\ 0 & -\delta \end{bmatrix} \quad (28)$$

and \hat{I} is identity matrix. In these equations, ρ_A and ρ_B represent the optical coherences corresponding to the transitions $|0\rangle \leftrightarrow |A\rangle$ and $|0\rangle \leftrightarrow |B\rangle$, respectively [which appear in Eq. (25) for the induced torque], whereas ρ_1 and ρ_2 denote the ground-state coherences between $|0\rangle$ and $|1\rangle$ as well as $|0\rangle$ and $|2\rangle$. The parameter Γ represents the spontaneous decay rate of the excited states, while δ and Δ correspond to the two-photon detuning and probe detuning, respectively.

In what follows, we focus on the case where the four control fields have equal amplitudes Ω , allowing the complex Rabi frequencies to be written as

$$\Omega_i = \Omega e^{i\phi_i}, \quad i = A1, A2, B1, B2, \quad (29)$$

with ϕ_i representing the phase of each field. To derive the optical Bloch equations, we assume that the probe fields are significantly weaker than the control fields, ensuring that the atomic population remains predominantly in the ground state $|0\rangle$. This allows us to treat the probe fields as a perturbation. Furthermore, all rapidly oscillating exponential factors related to the central frequencies and wave vectors have been removed, leaving only the slowly varying amplitudes. This is justified under the SVEA and RWA, which assume that the field envelopes vary slowly in space and time compared to the optical wavelength and period, so that the rapidly oscillating terms average to zero.

We seek the steady-state solutions of the probe fields Ω_{A0} and Ω_{B0} by dropping the time derivatives in Eqs. (26) and (27) (i.e., when $\frac{\partial}{\partial t} \rightarrow 0$). This corresponds to the long-term behavior of the optical coherences ρ_A and ρ_B . From Eq. (27) we obtain

$$\begin{bmatrix} \rho_1 \\ \rho_2 \end{bmatrix} = -(\Delta\hat{I} + \hat{\delta})^{-1} \hat{\Omega}^\dagger \begin{bmatrix} \rho_A \\ \rho_B \end{bmatrix}. \quad (30)$$

Substituting this expression into Eq. (26) yields

$$\hat{\Omega}(\Delta\hat{I} + \hat{\delta})^{-1} \hat{\Omega}^\dagger \begin{bmatrix} \rho_A \\ \rho_B \end{bmatrix} - \left(\Delta + i\frac{\Gamma}{2} \right) \begin{bmatrix} \rho_A \\ \rho_B \end{bmatrix} = \begin{bmatrix} \Omega_{A0} \\ \Omega_{B0} \end{bmatrix}. \quad (31)$$

Rearranging Eq. (31), we obtain the steady-state solutions for ρ_A and ρ_B ,

$$\begin{bmatrix} \rho_A \\ \rho_B \end{bmatrix} = \left[\hat{\Omega}(\Delta\hat{I} + \hat{\delta})^{-1} \hat{\Omega}^\dagger - \left(\Delta + i\frac{\Gamma}{2} \right) \hat{I} \right]^{-1} \begin{bmatrix} \Omega_{A0} \\ \Omega_{B0} \end{bmatrix}. \quad (32)$$

III. PHASE-SENSITIVE TORQUE

Equations (25), (28), and (32) collectively indicate that the variation of torque function τ depends on the Rabi frequency Ω as well as the two-photon detuning δ . However, these expressions do not explicitly reveal the dependence on the relative phase ϕ between the applied fields. In the following,

we will show this phase dependence by considering different cases of light-matter interaction.

A. Nonzero two-photon detuning $\delta \neq 0$

For nonzero two-photon detuning $\delta \neq 0$ and equal control field amplitudes Ω , we simplify the inverse term in Eq. (32) using Eqs. (28) and (29) as

$$\hat{\Omega}(\Delta\hat{I} + \hat{\delta})^{-1}\hat{\Omega}^\dagger = \frac{2\Omega^2\Delta}{\Delta^2 - \delta^2} \begin{bmatrix} 1 & e^{i(\theta+\phi/2)}[\cos(\frac{\phi}{2}) - i\frac{\delta}{\Delta}\sin(\frac{\phi}{2})] \\ e^{-i(\theta+\phi/2)}[\cos(\frac{\phi}{2}) + i\frac{\delta}{\Delta}\sin(\frac{\phi}{2})] & 1 \end{bmatrix}, \quad (33)$$

where $\phi = (\phi_{A1} - \phi_{B1}) - \theta$ and $\theta = \phi_{A2} - \phi_{B2}$. Here ϕ represents the total relative phase among all four control fields and θ provides an additional (phase) degree of control over the optical torque exerted on the DT system. Substituting Eq. (33) into Eq. (32) yields the optical coherence vector

$$\begin{bmatrix} \rho_A \\ \rho_B \end{bmatrix} = \frac{\frac{\Delta^2 - \delta^2}{2\Omega^2\Delta^2}}{\left(1 - \frac{(\Delta^2 - \delta^2)(2\Delta + i\Gamma)}{4\Omega^2\Delta}\right)^2 - \cos^2(\frac{\phi}{2}) - \frac{\delta^2}{\Delta^2}\sin^2(\frac{\phi}{2})} \times \begin{bmatrix} \Delta - \frac{(\Delta^2 - \delta^2)(2\Delta + i\Gamma)}{4\Omega^2} & -\Delta e^{i(\theta+\phi/2)}[\cos(\frac{\phi}{2}) - i\frac{\delta}{\Delta}\sin(\frac{\phi}{2})] \\ -\Delta e^{-i(\theta+\phi/2)}[\cos(\frac{\phi}{2}) + i\frac{\delta}{\Delta}\sin(\frac{\phi}{2})] & \Delta - \frac{(\Delta^2 - \delta^2)(2\Delta + i\Gamma)}{4\Omega^2} \end{bmatrix} \begin{bmatrix} \Omega_{A0} \\ \Omega_{B0} \end{bmatrix}. \quad (34)$$

1. Relative phase $\phi = \pi$

A particularly instructive scenario arises when the applied fields have a relative phase of π . By setting the phases of individual control fields to $(\phi_{A1}, \phi_{B1}, \phi_{A2}, \phi_{B2}) = (\pi, 0, 0, 0)$, we immediately have $\phi = \pi$ and $\theta = 0$. In this case, the system undergoes a reorganization due to phase-controlled interference. The π -phase difference rotates the bright-dark basis in Eqs. (2)–(5) into symmetric and antisymmetric superpositions of

$$|\mathcal{B}_A\rangle = \frac{\Omega e^{i\pi}|1\rangle + \Omega|2\rangle}{\sqrt{2}\Omega} = \frac{|2\rangle - |1\rangle}{\sqrt{2}} \rightarrow |-\rangle, \quad (35)$$

$$|\mathcal{D}_A\rangle = \frac{|1\rangle + |2\rangle}{\sqrt{2}} \rightarrow |+\rangle \quad (36)$$

$$|\mathcal{B}_B\rangle = \frac{\Omega|1\rangle + \Omega|2\rangle}{\sqrt{2}\Omega} = \frac{|1\rangle + |2\rangle}{\sqrt{2}} \rightarrow |+\rangle \quad (37)$$

$$|\mathcal{D}_B\rangle = \frac{|1\rangle - |2\rangle}{\sqrt{2}} \rightarrow |-\rangle. \quad (38)$$

Note that the “flip” between $\frac{|2\rangle - |1\rangle}{\sqrt{2}}$ and $\frac{|1\rangle - |2\rangle}{\sqrt{2}}$ is just an unobservable global minus sign; thus both conventions represent the same antisymmetric state.

In addition, Eqs. (7)–(9) yield $C_B = C_D = 0$ and $C_X = 1$, simplifying the Hamiltonian in Eq. (6) to

$$H = (-\varepsilon_A|A\rangle\langle 0| - \varepsilon_B|B\rangle\langle 0| - \Omega_A|A\rangle\langle -| - \Omega_B|B\rangle\langle +| + \text{H.c.} - \delta(|+\rangle\langle -| + |-\rangle\langle +|)). \quad (39)$$

This indicates that the applied π -phase difference leads to coupling between $|A\rangle$ and the antisymmetric $|-\rangle$ state and between $|B\rangle$ and the symmetric state $|+\rangle$. The control fields driving these transitions are renormalized into effective couplings with Rabi frequencies $\Omega_A = \Omega_B = \sqrt{2}\Omega$, a result of constructive interference in the transformed basis. This

transformation reconfigures the DT system into two coupled- Λ subsystems [Fig. 1 (b)]. The first Λ subsystem involves transitions $|0\rangle \leftrightarrow |A\rangle \leftrightarrow |-\rangle$, while the second involves $|0\rangle \leftrightarrow |B\rangle \leftrightarrow |+\rangle$. The term δ introduces crosstalk between two Λ subsystems.

Under this condition, Eq. (34) simplifies to

$$\begin{bmatrix} \rho_A \\ \rho_B \end{bmatrix} = \frac{8\Omega^2}{[4\Omega^2 - (2\Delta + i\Gamma)(\Delta + \delta)][4\Omega^2 - (2\Delta + i\Gamma)(\Delta - \delta)]} \times \begin{bmatrix} \Delta - \frac{(\Delta^2 - \delta^2)(2\Delta + i\Gamma)}{4\Omega^2} & -\delta \\ -\delta & \Delta - \frac{(\Delta^2 - \delta^2)(2\Delta + i\Gamma)}{4\Omega^2} \end{bmatrix} \begin{bmatrix} \Omega_{A0} \\ \Omega_{B0} \end{bmatrix}. \quad (40)$$

The off-diagonal term $-\delta$ explicitly couples the two probe fields Ω_{A0} and Ω_{B0} . This two-photon detuning-mediated interaction leads to a phase-sensitive coupling, which directly affects both the optical response of the system and its mechanical dynamics.

Figure 2 illustrates the induced torque τ as a function of the probe detuning Δ for different values of δ : $\delta = \Gamma$, 2Γ , and 3Γ in Figs. 2(a), 2(b), and 2(c) and $\delta = -\Gamma$, -2Γ , and -3Γ in Figs. 2(d), 2(e), and 2(f), respectively. In all cases, we consider equal probe amplitudes $|\Omega_{A0}| = |\Omega_{B0}|$. As defined in Eq. (25), the torque function corresponds to the sum of the imaginary parts of the coherences ρ_A and ρ_B , which are associated with the absorption of the probe fields Ω_{A0} and Ω_{B0} . Consequently, the torque profile resembles the absorption spectrum of the probe fields. As shown in Fig. 2, the torque exhibits peaks on either side of $\Delta = \delta$, which corresponds to the condition where the system exhibits EIT for both probe fields. According to Eq. (40), when $|\Omega_{A0}| = |\Omega_{B0}|$, the coherence terms ρ_A and ρ_B (and thus their imaginary parts) vanish at $\Delta = \delta$, leading to

transparency. Adjusting the two-photon detuning δ shifts the EIT window for both probes and thereby changes the position and width of the torque peaks. For instance, when $\delta = \Gamma$ [Fig. 2(a)], while for $\delta = -\Gamma$, the transparency window shifts to $\Delta = -\Gamma$ [Fig. 2(d)]. Increasing δ to larger positive (negative) values gradually broadens the left (right) torque peak. This behavior confirms that the torque is rooted in absorptive processes: When EIT suppresses

$$\begin{aligned} (\phi_{A1}, \phi_{B1}, \phi_{A2}, \phi_{B2}) &= \left(\frac{\pi}{2}, 0, 0, \frac{\pi}{2}\right) \Rightarrow \phi = \pi, \quad \theta = -\pi/2 \quad [\text{phase (a)}], \\ (\phi_{A1}, \phi_{B1}, \phi_{A2}, \phi_{B2}) &= \left(\frac{\pi}{6}, 0, 0, \frac{5\pi}{6}\right) \Rightarrow \phi = \pi, \quad \theta = -5\pi/6 \quad [\text{phase (b)}], \\ (\phi_{A1}, \phi_{B1}, \phi_{A2}, \phi_{B2}) &= \left(\frac{\pi}{3}, 0, 0, \frac{2\pi}{3}\right) \Rightarrow \phi = \pi, \quad \theta = -2\pi/3 \quad [\text{phase (c)}], \\ (\phi_{A1}, \phi_{B1}, \phi_{A2}, \phi_{B2}) &= \left(\frac{5\pi}{6}, 0, 0, \frac{\pi}{6}\right) \Rightarrow \phi = \pi, \quad \theta = -\pi/6 \quad [\text{phase (d)}]. \end{aligned} \quad (41)$$

Despite ϕ being constant, variations in θ redistribute the torque variation (Fig. 3), revealing θ as an independent control parameter. From Eq. (34), the off-diagonal elements of the response matrix governing ρ_A and ρ_B include terms of the form $e^{\pm i(\theta + \phi/2)}$. Therefore, even when $\phi = \pi$, tuning θ adjusts the phase difference between the $|A\rangle$ - and $|B\rangle$ -mediated pathways, thereby altering the interference conditions. This phase-dependent interference directly impacts the imaginary parts of the coherences ρ_A and ρ_B , which are responsible for the torque generation. For instance, the case $\theta = -\frac{\pi}{2}$ [Fig. 3(a)] results in four pronounced torque

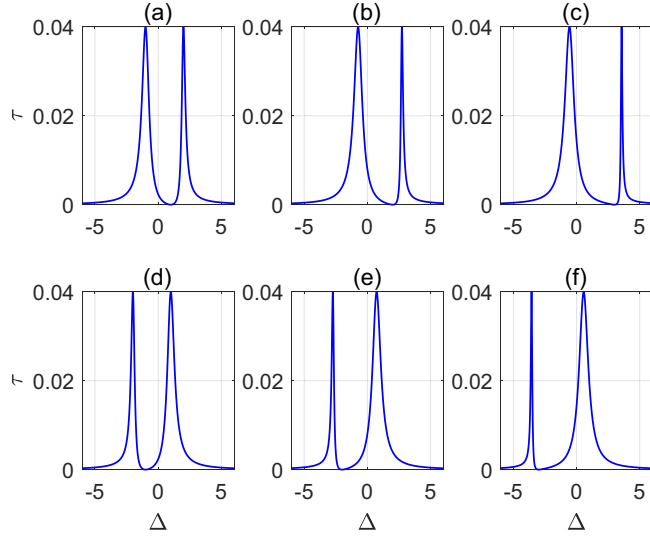


FIG. 2. Induced torque function τ as a function of probe detuning Δ at nonzero two-photon detuning for (a) $\delta = \Gamma$, (b) $\delta = 2\Gamma$, (c) $\delta = 3\Gamma$, (d) $\delta = -\Gamma$, (e) $\delta = -2\Gamma$, and (f) $\delta = -3\Gamma$. The strength of probe fields are $|\Omega_{A0}| = |\Omega_{B0}| = 0.1\Gamma$. The amplitudes of the individual control fields are $|\Omega_{A1}| = |\Omega_{A2}| = |\Omega_{B1}| = |\Omega_{B2}| = |\Omega| = \Gamma$. The phases of the individual control fields are set as $(\phi_{A1}, \phi_{B1}, \phi_{A2}, \phi_{B2}) = (\pi, 0, 0, 0)$, leading to $\phi = \pi$ and $\theta = 0$, which simplifies the DT system to two coupled- Λ systems. All the relevant parameters are scaled with Γ .

absorption, the torque vanishes; when absorption is enhanced near resonance, the torque reaches its peak and reflects the transfer of OAM from the twisted light fields to the DT atoms.

To isolate the role of the emergent phase θ on the induced torque, we fix $\phi = \pi$ and vary θ by adjusting the control field phases. Specifically, we consider four different phase configurations for the control fields:

peaks, reflecting constructive interference between the two pathways.

2. Relative phase $\phi = 0$

Next we consider the case where all control field phases are set to zero $(\phi_{A1}, \phi_{B1}, \phi_{A2}, \phi_{B2}) = (0, 0, 0, 0)$, yielding $\phi = 0, \theta = 0$. From Eqs. (2)–(5) it follows that the bright states

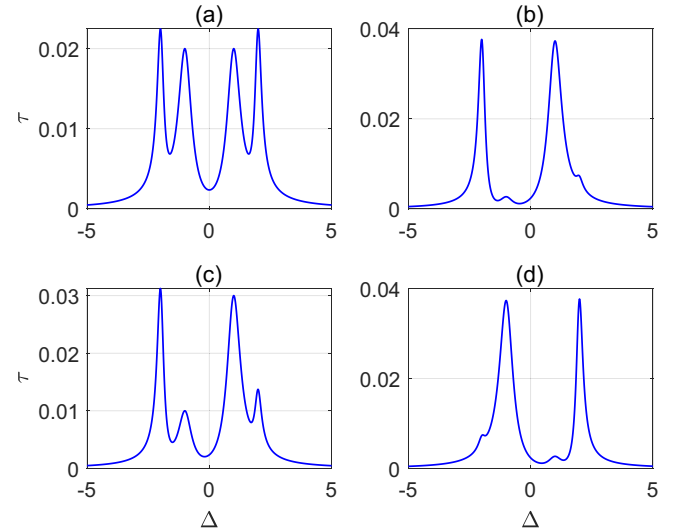


FIG. 3. Induced torque function τ as a function of probe detuning Δ at nonzero two-photon detuning $\delta = \Gamma$ for different values of additional phase θ . The strengths of the probe fields are $|\Omega_{A0}| = |\Omega_{B0}| = 0.1\Gamma$. The amplitudes of the individual control fields are $|\Omega_{A1}| = |\Omega_{A2}| = |\Omega_{B1}| = |\Omega_{B2}| = |\Omega| = \Gamma$. The phases of the individual control fields are set as (a) $(\phi_{A1}, \phi_{B1}, \phi_{A2}, \phi_{B2}) = (\frac{\pi}{2}, 0, 0, \frac{\pi}{2})$, leading to $\phi = \pi$ and $\theta = -\pi/2$; (b) $(\phi_{A1}, \phi_{B1}, \phi_{A2}, \phi_{B2}) = (\frac{\pi}{6}, 0, 0, \frac{5\pi}{6})$, leading to $\phi = \pi$ and $\theta = -5\pi/6$; (c) $(\phi_{A1}, \phi_{B1}, \phi_{A2}, \phi_{B2}) = (\frac{\pi}{3}, 0, 0, \frac{2\pi}{3})$, leading to $\phi = \pi$ and $\theta = -2\pi/3$; and (d) $(\phi_{A1}, \phi_{B1}, \phi_{A2}, \phi_{B2}) = (\frac{5\pi}{6}, 0, 0, \frac{\pi}{6})$, leading to $\phi = \pi$ and $\theta = -\pi/6$.

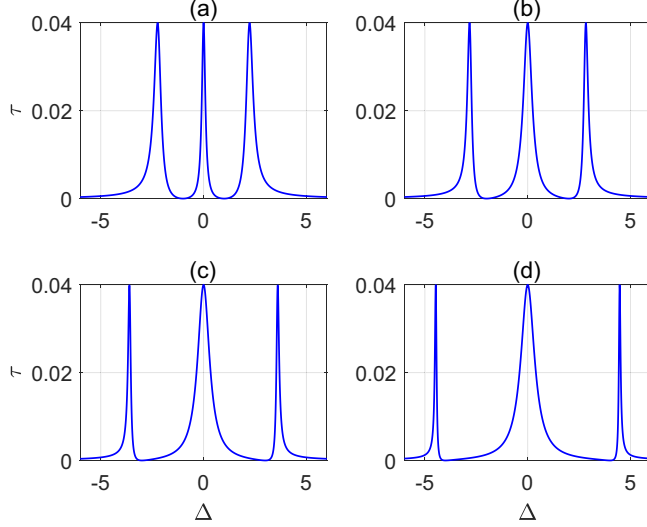


FIG. 4. Induced torque function τ as a function of probe detuning Δ at nonzero two-photon detuning (a) $\delta = \Gamma$, (b) $\delta = 2\Gamma$, (c) $\delta = 3\Gamma$, and (d) $\delta = 4\Gamma$. The strength of probe fields are $|\Omega_{A0}| = |\Omega_{B0}| = 0.1\Gamma$. The amplitudes of the individual control fields are $|\Omega_{A1}| = |\Omega_{A2}| = |\Omega_{B1}| = |\Omega_{B2}| = |\Omega| = \Gamma$. The phases of the individual control fields are set as $(\phi_{A1}, \phi_{B1}, \phi_{A2}, \phi_{B2}) = (0, 0, 0, 0)$, leading to $\phi = \theta = 0$, which simplifies the DT system to a DL system combined with two ground levels with no light (degenerate DT system).

$|\mathcal{B}_A\rangle$ and $|\mathcal{B}_B\rangle$ collapse into a single symmetric superposition

$$|\mathcal{B}_A\rangle = |\mathcal{B}_B\rangle = \frac{|1\rangle + |2\rangle}{\sqrt{2}} \rightarrow |+\rangle, \quad (42)$$

while the dark states become $|\mathcal{D}_A\rangle, |\mathcal{D}_B\rangle \rightarrow |-\rangle$. In this transformed basis, the Hamiltonian becomes

$$\begin{aligned} H = & (-\varepsilon_A |A\rangle\langle 0| - \varepsilon_B |B\rangle\langle 0| - \Omega_A |A\rangle\langle +| - \Omega_B |B\rangle\langle +| \\ & + \text{H.c.} + \delta(|+\rangle\langle -| + |-\rangle\langle +|)). \end{aligned} \quad (43)$$

This configuration couples both excited states $|A\rangle$ and $|B\rangle$ to the same symmetric ground-state superposition $|+\rangle$, forming two Λ subsystems $|0\rangle \leftrightarrow |A\rangle \leftrightarrow |+\rangle$ and $|0\rangle \leftrightarrow |B\rangle \leftrightarrow |+\rangle$. As a result, the DT configuration effectively reduces to a double- Λ (DL) structure [Fig. 1(c)], with coherent coupling between the DL structure and the antisymmetric state $|-\rangle$ mediated by the two-photon detuning δ .

Equation (34) now takes the form

$$\begin{bmatrix} \rho_A \\ \rho_B \end{bmatrix} = \frac{-2}{\Delta(2\Delta + i\Gamma)(2 - \frac{(\Delta^2 - \delta^2)(2\Delta + i\Gamma)}{4\Omega^2\Delta})} \times \begin{bmatrix} \Delta - \frac{(\Delta^2 - \delta^2)(2\Delta + i\Gamma)}{4\Omega^2} & -\Delta \\ -\Delta & \Delta - \frac{(\Delta^2 - \delta^2)(2\Delta + i\Gamma)}{4\Omega^2} \end{bmatrix} \begin{bmatrix} \Omega_{A0} \\ \Omega_{B0} \end{bmatrix}. \quad (44)$$

The torque function τ is plotted as a function of probe detuning Δ for different values of $\delta = \Gamma, 2\Gamma, 3\Gamma$, and 4Γ in Fig. 4. The system now exhibits three distinct peaks in the torque profile, which surround two EIT channels located at $\Delta = \pm\delta$ for both probe fields. This behavior follows directly

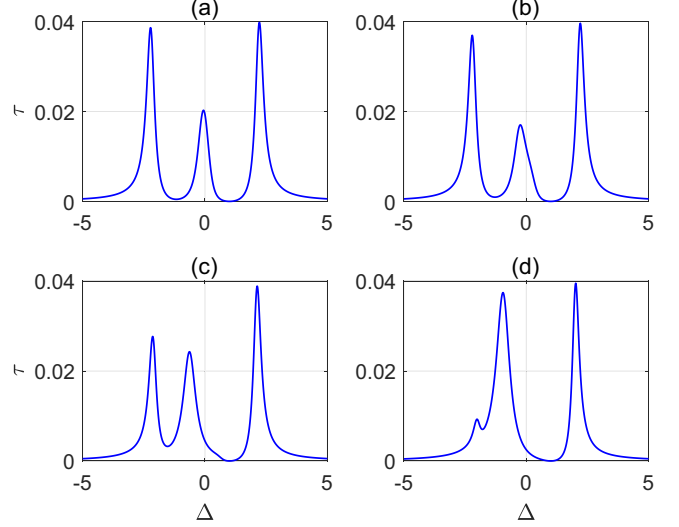


FIG. 5. Induced torque function τ as a function of probe detuning Δ , evaluated at nonzero two-photon detuning $\delta = \Gamma$ for different values of the relative phase ϕ . The strengths of the probe fields are $|\Omega_{A0}| = |\Omega_{B0}| = 0.1\Gamma$ and the amplitudes of the individual control fields are $|\Omega_{A1}| = |\Omega_{A2}| = |\Omega_{B1}| = |\Omega_{B2}| = |\Omega| = \Gamma$. The phases of the control fields $(\phi_{A1}, \phi_{B1}, \phi_{A2}, \phi_{B2})$ are set as (a) $(\frac{\pi}{6}, 0, 0, 0)$, (b) $(\frac{\pi}{4}, 0, 0, 0)$, (c) $(\frac{\pi}{2}, 0, 0, 0)$, and (d) $(\frac{5\pi}{6}, 0, 0, 0)$, corresponding to different values of $\phi = \phi_{A1}$ with $\theta = 0$.

from the diagonal terms of the coherence matrix in Eq. (44), which vanish when $|\Omega_{A0}| = |\Omega_{B0}|$, and the probe detuning satisfies $\Delta^2 - \delta^2 = 0$. Increasing the two-photon detuning δ broadens the central torque peak while sharpening the two lateral peaks. This is because the EIT windows shift further apart as δ increases, occurring at $\pm\delta = \Gamma, 2\Gamma, 3\Gamma$, and 4Γ . These peaks correspond to enhanced OAM transfer from the helical phase gradients of the LG probe fields to atoms.

3. Intermediate relative phases $0 < \phi < \pi$

Figure 5 illustrates the influence of the intermediate relative phase values ϕ ($0 < \phi < \pi$) on the torque spectrum for a fixed $\theta = 0$. Unlike the symmetric torque profile observed for $\phi = \pi$ (Fig. 2) and $\phi = 0$ (Fig. 4), a nonzero ϕ introduces a pronounced asymmetry. As ϕ increases, the left torque peak gradually diminishes and eventually merges with the central peak, while the right peak remains relatively stable. This asymmetry arises from phase-sensitive interference in the coherence terms ρ_A and ρ_B given in Eq. (34). Their imaginary parts, which govern the torque response, include complex phase-dependent factors of the form $e^{\pm i\phi/2}(\cos \frac{\phi}{2} \mp i \frac{\delta}{\Delta} \sin \frac{\phi}{2})$. These expressions show that variations in ϕ modulate both the relative amplitudes and phases of the atomic coherences. As a result, the interference conditions are altered across the spectrum, leading to a redistribution of peak intensities and the emergence of the observed torque asymmetry.

B. Zero two-photon detuning $\delta = 0$

Thus far we have considered the case of nonzero two-photon detuning. Let us now consider a situation when the two-photon detuning is zero $\delta = 0$. For $\phi = \pi$, the coherence

matrix simplifies considerably:

$$\begin{bmatrix} \rho_A \\ \rho_B \end{bmatrix} = \frac{8\Omega^2}{[4\Omega^2 - \Delta(2\Delta + i\Gamma)]^2} \times \begin{bmatrix} \Delta - \frac{\Delta^2(2\Delta+i\Gamma)}{4\Omega^2} & 0 \\ 0 & \Delta - \frac{\Delta^2(2\Delta+i\Gamma)}{4\Omega^2} \end{bmatrix} \begin{bmatrix} \Omega_{A0} \\ \Omega_{B0} \end{bmatrix}. \quad (45)$$

In this case, the off-diagonal terms in the coherence matrix vanish and the DT system reduces to a situation where the two probe fields are completely decoupled. Under these conditions, the DT configuration behaves as two independent Λ -type systems (or equivalently as two uncoupled EIT channels). The π -phase difference in the control fields reorganizes the ground states $|1\rangle$ and $|2\rangle$ into the orthogonal superpositions $|+\rangle = \frac{|1\rangle+|2\rangle}{\sqrt{2}}$ and $|-\rangle = \frac{|1\rangle-|2\rangle}{\sqrt{2}}$. Thus, each probe field interacts with its respective superposition state, splitting the system into two distinct Λ subsystems.

For $\delta = 0$, setting $\phi_{A1} = \phi_{B1} = \phi_{A2} = \phi_{B2} = 0$ results in the overall relative phase $\phi = \theta = 0$. In this case, the coherence terms take the form

$$\begin{bmatrix} \rho_A \\ \rho_B \end{bmatrix} = \frac{-2}{\Delta(2\Delta + i\Gamma)(2 - \frac{\Delta(2\Delta+i\Gamma)}{4\Omega^2})} \times \begin{bmatrix} \Delta - \frac{\Delta^2(2\Delta+i\Gamma)}{4\Omega^2} & -\Delta \\ -\Delta & \Delta - \frac{\Delta^2(2\Delta+i\Gamma)}{4\Omega^2} \end{bmatrix} \begin{bmatrix} \Omega_{A0} \\ \Omega_{B0} \end{bmatrix}. \quad (46)$$

This corresponds to a symmetric (degenerate) double- Λ configuration. The nonzero off-diagonal terms in the coherence matrix introduce coupling between the two probe fields. This coupling induces interference between the imaginary parts of ρ_A and ρ_B which govern the torque. The resulting torque variations are illustrated in Fig. 6. The torque exhibits an absorptionlike profile: It vanishes at the center due to EIT, while reaching maxima on either side as a result of enhanced absorption. In the case of $\phi = \pi$, shown in Fig. 6(a), the absence of probe coupling suppresses the joint interaction between the two probe fields. This modifies the spectral torque response, leading to a reduced separation between the torque extrema.

Before concluding, we note that in optical beams carrying OAM, a macroscopic particle can experience a spinning torque that causes it to rotate about its own axis [36,37]. In contrast, in our model each atom is treated as a pointlike particle on which the force acts individually. Therefore, a spinning torque on a single atom is not defined. Our analysis considers only the orbital torque, which induces rotational motion of the atomic center of mass around the beam axis. Since the atomic ensemble is not treated as a rigid body, no collective spinning motion is expected.

IV. SUMMARY

We demonstrated theoretically phase-controllable optical torque in a five-level double-tripod atomic system driven by four strong coherent control fields and two weak optical vortex probe fields carrying orbital angular momentum. The spatial phase gradients of the OAM fields induce a quantized

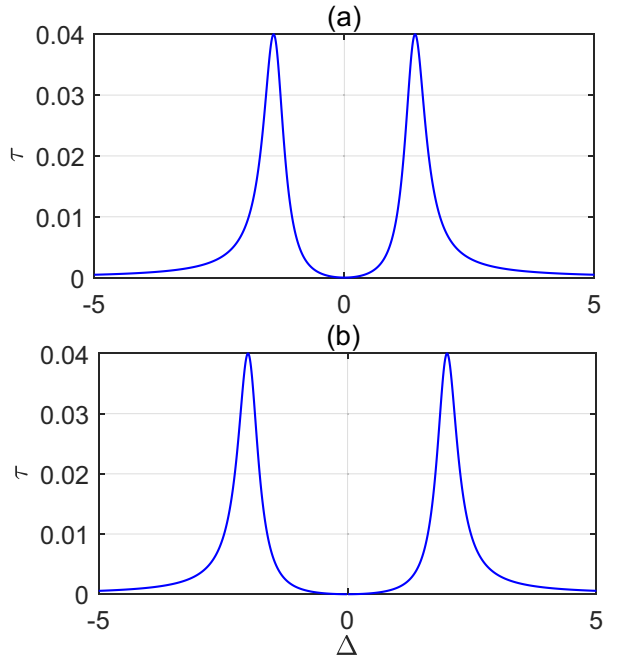


FIG. 6. Torque function τ as a function of probe detuning Δ at zero two-photon detuning $\delta = 0$ and for different values of relative phase ϕ . The strength of probe fields are $|\Omega_{A0}| = |\Omega_{B0}| = 0.1\Gamma$. The amplitudes of the individual control fields are $|\Omega_{A1}| = |\Omega_{A2}| = |\Omega_{B1}| = |\Omega_{B2}| = |\Omega| = \Gamma$. The phases of the individual control fields are set as $\phi_{B1} = \phi_{A2} = \phi_{B2} = 0$ and (a) $\phi_{A1} = \pi$ and (b) 0 (leading to $\phi = \phi_{A1}$ and $\theta = 0$).

torque, transferred to atoms to drive rotational motion and directed atomic flow in an annular geometry. By analytically solving the optical Bloch equations in steady state, we revealed that both the torque and resultant rotation exhibit high phase sensitivity, arising from coherent reconfigurations of the system into either coupled- Λ or double- Λ configurations depending on the relative phases ϕ and θ of the control fields. Each configuration displays distinct torque characteristics. The multilevel DT configuration explored here represents a highly flexible setup, which allows employing several degrees of freedom to get different torque effects not available using simpler systems. Indeed, here the control over the total relative phase ϕ , extra phase θ , and two-photon detuning δ can be used, affecting the overall torque behavior and rotation dynamics. Moreover, we emphasized that the observed toroidal atomic currents and related annular geometry effects are specifically related to the annular intensity distribution of the vortex probe beams. This phase-controlled light-induced torque establishes a versatile mechanism for optical manipulation of quantized mechanical action in multilevel atomic ensembles.

In the present model, the control fields are assumed to be spatially uniform, and the optical torque arises from the spatial phase gradients of the probe fields carrying OAM. Recent studies have demonstrated that spatial variations in the field amplitude can significantly influence Rabi oscillations and spin-orbit-coupling effects in structured light fields [38,39]. This indicates that the induced torque could in principle be controlled through both the spatial amplitude

and phase profiles of a vortex control field. If the control fields were also spatially structured in our DT system, their amplitude distribution and OAM phase could introduce additional torque components. However, not all control fields can simultaneously carry vortices in the DT configuration, as this would lead to a central intensity minimum (“hole”) and may cause nonadiabatic losses in the dark-state coherence. Therefore, in the present work we restrict the control fields to vortex-free configurations, while the OAM-induced torque originates solely from the probe beams. The extension of the model to include spatially structured control fields will be an interesting direction for future work.

The DT atomic system can be realized experimentally in cold ^{87}Rb , where the atomic population is first prepared in a single Zeeman sublevel. This can be accomplished by applying strong σ^+ laser fields driving the transitions from the ground hyperfine states $|F = 1\rangle$ and $|F = 2\rangle$ to the excited states $|F' = 2\rangle$ and $|F'' = 2\rangle$, corresponding to the $|5S_{1/2}\rangle$, $|5P_{1/2}\rangle$, and $|5P_{3/2}\rangle$ manifolds, respectively. Under these pumping conditions, the Zeeman sublevel $|F = 2, m = 2\rangle$ will

be the only dark ground state, and optical pumping transfers the entire population into this state. Two probe fields drive the transitions $|F = 2\rangle \rightarrow |F' = 2\rangle$ and $|F = 2\rangle \rightarrow |F'' = 2\rangle$ with σ^- polarization. Since all other ground-state Zeeman sublevels remain unpopulated, the only relevant probe transitions are $|F = 2, m = 2\rangle \rightarrow |F' = 2, m = 1\rangle$ and $|F = 2, m = 2\rangle \rightarrow |F'' = 2, m = 1\rangle$. This produces the DT coupling configuration shown in Fig. 1, with no significant contribution from other states or transitions.

ACKNOWLEDGMENT

This work received funding from the Research Council of Lithuania (LMTLT), Grant Agreement No. S-ITP-24-6.

DATA AVAILABILITY

The data that support the findings of this article are not publicly available. The data are available from the authors upon reasonable request.

-
- [1] D. F. Walls and G. J. Milburn, *Quantum Optics* (Springer, Berlin, 1994).
 - [2] M. O. Scully and M. S. Zubairy, *Quantum Optics* (Cambridge University Press, Cambridge, 1997).
 - [3] P. Meystre, *Atom Optics* (Springer, New York, 2001).
 - [4] J. R. Anglin and W. Ketterle, Bose-Einstein condensation of atomic gases, *Nature (London)* **416**, 211 (2002).
 - [5] S. E. Harris, Electromagnetically induced transparency, *Phys. Today* **50**(7), 36 (1997).
 - [6] M. D. Lukin, *Colloquium: Trapping and manipulating photon states in atomic ensembles*, *Rev. Mod. Phys.* **75**, 457 (2003).
 - [7] M. Fleischhauer, A. Imamoglu, and J. P. Marangos, Electromagnetically induced transparency: Optics in coherent media, *Rev. Mod. Phys.* **77**, 633 (2005).
 - [8] J. Zhang, G. Hernandez, and Y. Zhu, Slow light with cavity electromagnetically induced transparency, *Opt. Lett.* **33**, 46 (2008).
 - [9] G. Juzeliūnas and H. J. Carmichael, Systematic formulation of slow polaritons in atomic gases, *Phys. Rev. A* **65**, 021601(R) (2002).
 - [10] G. Juzeliūnas and P. Öhberg, Slow light in degenerate Fermi gases, *Phys. Rev. Lett.* **93**, 033602 (2004).
 - [11] M.-J. Lee, J. Ruseckas, C.-Y. Lee, V. Kudriāšov, K.-F. Chang, H.-W. Cho, G. Juzeliūnas, and I. A. Yu, Experimental demonstration of spinor slow light, *Nat. Commun.* **5**, 5542 (2014).
 - [12] J. D. Sivers, J. Hannegan, and Q. Quraishi, Demonstration of slow light in rubidium vapor using single photons from a trapped ion, *Sci. Adv.* **5**, eaav4651 (2019).
 - [13] M. D. Lukin, S. F. Yelin, and M. Fleischhauer, Entanglement of atomic ensembles by trapping correlated photon states, *Phys. Rev. Lett.* **84**, 4232 (2000).
 - [14] M. Fleischhauer and M. D. Lukin, Dark-state polaritons in electromagnetically induced transparency, *Phys. Rev. Lett.* **84**, 5094 (2000).
 - [15] H. R. Hamedi, J. Ruseckas, and G. Juzeliūnas, Electromagnetically induced transparency and nonlinear pulse propagation in a combined tripod and lambda atom-light coupling scheme, *J. Phys. B* **50**, 185401 (2017).
 - [16] E. Paspalakis and P. L. Knight, Electromagnetically induced transparency and controlled group velocity in a multilevel system, *Phys. Rev. A* **66**, 015802 (2002).
 - [17] Q.-Q. Bao, X.-H. Zhang, J.-Y. Gao, Y. Zhang, C.-L. Cui, and J.-H. Wu, Coherent generation and dynamic manipulation of double stationary light pulses in a five-level double-tripod system of cold atoms, *Phys. Rev. A* **84**, 063812 (2011).
 - [18] L. Allen, M. W. Beijersbergen, R. J. C. Spreeuw, and J. P. Woerdman, Orbital angular momentum of light and the transformation of Laguerre-Gaussian laser modes, *Phys. Rev. A* **45**, 8185 (1992).
 - [19] L. Allen, M. J. Padgett, and M. Babiker, The orbital angular momentum of light, *Prog. Opt.* **39**, 291 (1999).
 - [20] C. Yu and Z. Wang, Engineering helical phase via four-wave mixing in the ultraslow propagation regime, *Phys. Rev. A* **103**, 013518 (2021).
 - [21] N. Radwell, T. W. Clark, B. Piccirillo, S. M. Barnett, and S. Franke-Arnold, Spatially dependent electromagnetically induced transparency, *Phys. Rev. Lett.* **114**, 123603 (2015).
 - [22] H. R. Hamedi, V. Kudriāšov, J. Ruseckas, and G. Juzeliūnas, Azimuthal modulation of electromagnetically induced transparency using structured light, *Opt. Express* **26**, 28249 (2018).
 - [23] S. Sharma and T. N. Dey, Phase-induced transparency-mediated structured-beam generation in a closed-loop tripod configuration, *Phys. Rev. A* **96**, 033811 (2017).
 - [24] D. Akamatsu and M. Kozuma, Coherent transfer of orbital angular momentum from an atomic system to a light field, *Phys. Rev. A* **67**, 023803 (2003).
 - [25] J. Ruseckas, V. Kudriāšov, I. A. Yu, and G. Juzeliūnas, Transfer of orbital angular momentum of light using two-component slow light, *Phys. Rev. A* **87**, 053840 (2013).
 - [26] H. R. Hamedi, J. Ruseckas, and G. Juzeliūnas, Exchange of optical vortices using an electromagnetically-induced-transparency-based four-wave-mixing setup, *Phys. Rev. A* **98**, 013840 (2018).

- [27] H. R. Hamed, J. Ruseckas, E. Paspalakis, and G. Juzeliūnas, Off-axis optical vortices using double-Raman singlet and doublet light-matter schemes, *Phys. Rev. A* **101**, 063828 (2020).
- [28] F. Castellucci, T. W. Clark, A. Selyem, J. Wang, and S. Franke-Arnold, Atomic compass: Detecting 3D magnetic field alignment with vector vortex light, *Phys. Rev. Lett.* **127**, 233202 (2021).
- [29] M. Babiker, W. L. Power, and L. Allen, Light-induced torque on moving atoms, *Phys. Rev. Lett.* **73**, 1239 (1994).
- [30] M. F. Andersen, C. Ryu, P. Cladé, V. Natarajan, A. Vaziri, K. Helmerson, and W. D. Phillips, Quantized rotation of atoms from photons with orbital angular momentum, *Phys. Rev. Lett.* **97**, 170406 (2006).
- [31] V. E. Lembessis and M. Babiker, Light-induced torque for the generation of persistent current flow in atomic gas Bose-Einstein condensates, *Phys. Rev. A* **82**, 051402(R) (2010).
- [32] A. M. Yao and M. J. Padgett, Orbital angular momentum: Origins, behavior and applications, *Adv. Opt. Photonics* **3**, 161 (2011).
- [33] S. Liu, Y. Lou, and J. Jing, Orbital angular momentum multiplexed deterministic all-optical quantum teleportation, *Nat. Commun.* **11**, 3875 (2020).
- [34] M. Padgett and R. Bowman, Tweezers with a twist, *Nat. Photonics* **5**, 343 (2011).
- [35] R. J. Cook, Atomic motion in resonant radiation: An application of Ehrenfest's theorem, *Phys. Rev. A* **20**, 224 (1979).
- [36] Y. Hu, J. J. Kingsley-Smith, M. Nikkhou, J. A. Sabin, F. J. Rodriguez-Fortuno, X. Xu, and J. Millen, Structured transverse orbital angular momentum probed by a levitated optomechanical sensor, *Nat. Commun.* **14**, 2638 (2023).
- [37] X. Xu, M. Nieto-Vesperinas, Y. Zhou, Y. Zhang, M. Li, F. J. Rodriguez-Fortuno, S. Yan, and B. Yao, Gradient and curl optical torques, *Nat. Commun.* **15**, 6230 (2024).
- [38] G. Liu, X. Zhang, X. Zhang, Y. Hu, Z. Li, Z. Chen, and S. Fu, Spin-orbit Rabi oscillations in optically synthesized magnetic fields, *Light: Sci. Appl.* **12**, 205 (2023).
- [39] X. Zhang, G. Liu, Y. Hu, H. Lin, Z. Zeng, X. Zhang, Z. Li, Z. Chen, and S. Fu, Photonic spin-orbit coupling induced by deep-subwavelength structured light, *Phys. Rev. A* **109**, 023522 (2024).